

# On the quest of production of superheavy nuclei in reactions of $^{48}\text{Ca}$ with the heaviest actinide targets

P. Armbruster

GSI-Darmstadt, Planckstrasse 1, 64291 Darmstadt, Germany

Received: 13 October 1999

Communicated by B. Povh

**Abstract.** The sequence of radioactive decays of an unknown isotope produced in a rare fusion reaction to known lighter isotopes is used to identify mass and atomic number of the mother isotope, which has been separated before from the bulk of other reaction products by an in-flight recoil separator. By this technique the elements 107 to 112 were produced by single atom decay-chain analysis. Such a correlation technique reaches its limit by the occurrence of accidental sequences and it collapses beyond a maximum possible correlation time, at which a true event cannot be distinguished anymore from a random event.

$^{48}\text{Ca}$ -induced fusion reactions with actinides are discussed. In 1983 at GSI, Darmstadt and LBL, Berkeley,  $^{48}\text{Ca}/^{248}\text{Cm}$ -experiments (II) were performed, which are compared to recent  $^{48}\text{Ca}$ -experiments at FLNR-Dubna (I) irradiating  $^{244}\text{Pu}$ ,  $^{242}\text{Pu}$ , and  $^{238}\text{U}$ . In these experiments production of isotopes of superheavy elements 112 and 114 is claimed. Our analysis of accidental sequences in  $^{48}\text{Ca}$ -induced reactions is presented, which is at variance with the published analysis from FLNR-Dubna. We find that the maximum correlation time using continuous beams at today existing separation systems is not in the one-hour regime, but in the few-minute regime. The five spontaneous fission events observed in the FLNR experiments are preceded by signals in the (1–16)-minute range. These times are shown to be longer than the maximum possible correlation times. The preceding signals are decoupled from the spontaneous fission signal and carry no information on the spontaneous fission events observed. Moreover, random probabilities of 0.2 to 0.6 for the signals preceding the fission events indicate that the correlations are of random origin. The evidence to have discovered element 114 in the reported experiments is classified “very weak”.

**PACS.** 21.10.Dr Binding energies and masses – 23.60.+e  $\alpha$  decay – 25.70.-z Low and intermediate energy heavy-ion reactions – 27.90.+b  $220 \leq A$

## 1 Introduction

For the synthesis of superheavy elements two reaction mechanisms are used. In “cold fusion” medium weight n-rich projectiles  $Z > 20$  fused, with the closed-shell target nuclei  $^{208}\text{Pb}$  and  $^{209}\text{Bi}$  in 1n-reactions, have given the elements  $Z > 107$ –112. The hope is to reach finally  $Z = 113$ –115 [1–3]. In a very recent experiment at LBL Berkeley [4] three decay chains attributed to the reaction  $^{208}\text{Pb}(^{86}\text{Kr},n)^{293}118$  were observed extending the domain of “cold fusion” to  $Z = 118$ . However, until now this result could not be confirmed in an equally sensitive experiment at GSI. In “hot fusion” n-rich projectiles  $Z < 16$  fused, with the heaviest n-rich actinide targets in 4n- and 5n-reactions, have given isotopes of elements up to  $Z = 108$  [5]. Moreover, with  $^{48}\text{Ca}$ -projectiles in 3n-reactions the elements  $Z = 110$ –116 were envisaged [6–9]. Only these  $^{48}\text{Ca}$ -experiments are discussed in the following.

Today, world-wide the “One Atom/One New Element”-method, pioneered at GSI, is applied [10]. Single atoms of the new element are separated in-flight by a re-

coil spectrometer, and the element is identified from an analysis of the decay chain relating the new isotope to known isotopes. The decays in a sequence of generations are time-correlated to each other. As all correlation techniques the method is finally restricted by a maximum correlation time, beyond which accidental correlations dominate. Beyond this limit correlation analysis of sequences of signals is not allowed.

In three recent papers from FLNR, Dubna (I), [7–9], a claim of discovery of the isotopes  $^{289,287}114$ ,  $^{285,283}112$ ,  $^{281}110$ , and  $^{277}\text{Hs}$  in the reactions  $^{48}\text{Ca}/^{244,242}\text{Pu}$ ,  $^{238}\text{U}$  was made. In a former, less sensitive, but safer GSI/LBL-experiment in 1983 (II) no evidence for the production of superheavy elements in the reaction  $^{48}\text{Ca}/^{248}\text{Cm}$  could be found [6]. In this paper we point to the difficulty to apply correlation analysis to  $^{48}\text{Ca}$ -induced reactions at correlation times in the one-hour regime. Besides the fundamentals are presented, and the basic limitation of the “One Atom / One New Element”-method by random correlations is discussed. The hope is to exclude applications of the method to cases beyond its limits. Our group intro-

duced the method [10], and we want to show explicitly how to properly use it.

## 2 Three facts, $^{48}\text{Ca}$ on Actinide-reactions have to face

### 2.1 Spontaneous fission decays

There is a background of spontaneous fission activity found in irradiations of the heaviest actinide targets, which is not present in Pb/Bi-based reactions.  $^{238}\text{U}$ ,  $^{242,244}\text{Pu}$ ,  $^{248}\text{Cm}$  are close to the center of fission isomers and fission isomers produced as transfer products are entering the recoil spectrometers. In experiment (II) we observed one candidate for an uncorrelated spontaneous fission event. In the three recent experiments (I) altogether 10 spontaneous fission events were observed, two in [8] and four in [7, 9] each. For the system  $^{48}\text{Ca}/^{244}\text{Pu}$  at the Coulomb-barrier a value of 2 mb for the production of  $^{244}\text{Am}$  is expected. An isomer ratio of  $10^{-4}$  gives 200 nb production cross sections for the fission isomer. Even with the high suppression by the spectrometers in (I) of  $(2-5) \cdot 10^4$  [13] a few spontaneous fission events in 40 days, in good agreement with the experiments, are estimated to be detected behind the spectrometer. As  $^{244m}\text{Am}$  and  $^{241m}\text{Pu}$  have halfives of 0.9 ms and 24  $\mu\text{s}$ , respectively, short correlations to partners in the TOF-detector are to be expected, and in experiments [7, 9] two in each were actually found. The remaining 6 fission events had no signal in the TOF-detectors and 5 were assigned to another type of reaction, the effective cross section of which would be in the pb-regime as well. It was assumed that the five sf-events were residues from decay chains of superheavy nuclei, an hypothesis introduced ad hoc. Other less far reaching explanations should be considered and discarded. Small contaminations in the ppm-range of the actinide targets with Pb-isotopes could produce the spontaneously fissioning isotope  $^{252}\text{No}$  by fusion reactions. A measurement of the total kinetic energy of the fission products (TKE) in fission could discriminate between No and elements heavier than hassium. The spontaneous fission rates for  $^{248}\text{Cm}$  and higher targets increase, and the recoils implanted into the detector may fission themselves. This fission source becomes for  $^{248}\text{Cm}$ ,  $^{249}\text{Bk}$ , and  $^{249}\text{Cf}$  targets dominant. Finally, the transfer products themselves will fission, as  $^{256}\text{Cf}$  and  $^{256}\text{Fm}$ . Many new spontaneously fissioning isotopes were discovered starting from  $^{254}\text{Es}$  targets by this mechanism [14]. The fission events observed in the experiments (I and II) could stem from one of these known reactions, or even from  $^{252}\text{Cf}$  contaminations.

Appointing the 5 sf-events observed in experiments (I) to superheavy nuclei demands besides the sf-decay further information. Well-defined sequences of preceding non-random  $\alpha$ -correlations and a measurement of the high total kinetic energy released in the fission of the superheavy nucleus should corroborate the hypothesis. Three sf-events found in [7, 9] were reported to be correlated to (-decays, whereas in [8] the two spontaneous fission events were

correlated to an implanted recoil only. The TKE-values of  $(190 \pm 10)$  MeV measured are consistent with fission of  $Z = 96-100$ . To understand the origin of the fission events is crucial for the experiments (I). An explanation without the superheavy element-hypothesis discards all claims of element discovery. Fact is in the FNLR-experiments on the average every 15 days, or for  $3 \times 10^{18}$   $^{48}\text{Ca}$ -ions impinging on an actinide target, one fission event was observed in the implantation detector. It remains a challenge to find a method to determine from an isolated fission event the isotope of its origin.

### 2.2 Limitation of fusion in the entrance channel

The systematics of production cross sections of the heaviest elements revealed a trend to smaller and smaller cross sections [3, 5]. The price to be paid to reach the next higher element is a factor (3-4) in the production cross section. This trend is unbroken for “cold fusion” between  $Z = 102-112$ . Also, for “hot fusion” it is observed up to hassium, which was synthesized fusing  $^{34}\text{S}$  and  $^{238}\text{U}$  [5]. For “hot fusion” the cross sections were found for the heaviest elements to be smaller by 1 order of magnitude compared to “cold fusion”. No complete fusion reactions beyond a projectile mass of 34, that is for Ar- and Ca-projectiles on actinide targets, are confirmed outside of FLNR. The steady fall of cross sections is a phenomenon also established for fusion of mass symmetric collision partners [11]. The fall of cross-sections is explained by the increase of the ratio of Coulomb to nuclear forces with the atomic number. This macroscopic limitation of fusion in the entrance channel is expected to be general, and it limits the production of still higher atomic numbers most probably already before the ground-state stability of a superheavy nucleus falls beyond the experimental limit of detection in the range of  $\mu\text{s}$ -halfives [12]. The constant cross sections of a few pb given for all the latest experiments at FLNR trying to synthesize elements 110-114 are at variance with the accumulated data on fusion and the steady disappearance of evaporation residue formation by the increasing Coulomb repulsion in the entrance channel. The cross-sections derived from 1 or 2 correlation sequences found in the three FLNR experiments (I) cluster at the experimental limit of the facilities. Why does the cross-section in reactions of  $^{238}\text{U}$  with the projectiles  $^{26}\text{Mg}$  and  $^{34}\text{S}$  [5] covering four atomic numbers decrease by a factor of 100, and why should it stay constant for the same distance between  $^{34}\text{S}$  and  $^{48}\text{Ca}$  [8]? There must be a convincing cause, why the established decrease of cross-section disappears for  $^{48}\text{Ca}$ -reactions. A compensating stabilization of production cross sections in the order of a factor of 300 by decreasing evaporation losses of the compound system in 3n-reactions compared to 5n-reactions is proposed as a working hypothesis [7-9]. The quest for higher element is a challenge, but it stays imbedded in the firm knowledge of reaction mechanisms of the heaviest nuclei. This knowledge is not at disposal, and that is why strongly diverging cross-sections should be understood and investigated with care. The message they convey cannot be ignored, as is

done today in the rush for new elements. As no link to the world of known nuclei can be established for chains ending in sf-decay, at least the cross-sections could be linked to the world of known reaction mechanisms. Investigations covering collisions systems bridging the wide gap between the projectiles  $^{34}\text{S}$  and  $^{48}\text{Ca}$  are missing. They could have been the first step in the investigations and not the last one.

### 3 Multi-nucleon transfer reactions

In the  $^{48}\text{Ca}/^{248}\text{Cm}$ -experiment (II) element 116 was not found, but a very important discovery was made. Transfer reactions at the Coulomb-barrier fed with a total cross section larger than 30 mb, besides the more than 50 long-lived isotopes near the target nucleus, also about 45 short-lived  $\alpha$ -emitters in the mass range  $A = 210\text{--}230$  [15, 16]. 13 mb go into  $\alpha$ -particles from isotopes with half-lives less than a typical irradiation time of a month. Their activity is distributed about equally among the elements 83 to 92. For the  $^{48}\text{Ca}/^{244}\text{Pu}$ -reaction this cross section will not be very different. In the regime of disappearance of complete fusion and the onset of quasi-fission experiments on binary reactions [17, 18] confirmed the large cross-sections towards mass symmetry for multi-nucleon transfer reactions at the fusion barrier. For  $^{48}\text{Ca}$ -induced reactions on  $^{238}\text{U}$  at the barrier quasi-fission replacing complete fusion had become the dominant reaction channel, whereas for  $^{40}\text{Ca}$ -induced reactions complete fusion might still have occurred as a remnant reaction channel. Following these reaction studies the additional neutrons of  $^{48}\text{Ca}$  do not help to increase complete fusion in the entrance channel. Radiochemical studies comparing transfer reactions of  $^{40}\text{Ca}$ ,  $^{44}\text{Ca}$ , and  $^{48}\text{Ca}$  on  $^{248}\text{Cm}$  corroborated the dramatic change in reaction mechanism in the mass range  $A = (40 - 48)$ , away from complete fusion towards quasi-fission [19].

The successful discrimination of random correlations involving  $\alpha$ -particles emitted by transfer products was an important result in experiment (II). It was obtained by subdividing the detector in position sensitive pixels, by counting  $\alpha$ -particles and fission products during two third of the total measuring time in the pauses between beam pulses, and by using a detector system discriminating fusion events after the separation once more by their kinematics. As accidentals obey a rate equation the limits of the correlation method could be studied at the smaller luminosity of experiment (II), and the results can be transferred to the more sensitive experiments done today.

### 4 Three conditions underlying the “one atom/one new element”-method

In the following we give the basic equations to define a figure-of-merit for a separating device, to calculate the maximum possible correlation time  $t_{\max}$  for an experiment, and to estimate probabilities to find true events by

the correlation method. In the limit three conditions have to be fulfilled in order to identify a new element from the observation of a single nucleus and its decay chain using separation by a recoil separator equipped by a detector system, and analysis of time correlations between subsequent decays [10, 20].

- The product of beam intensity and the number of target atoms/cm<sup>2</sup>, that is the luminosity  $L$ , of the experimental set-up separating the wanted species with an efficiency  $\varepsilon_0$  should allow to synthesize in a measuring time  $T$  chosen and at a cross section  $\sigma_0$  envisaged, at least one event. This defines the first condition.

$$n = L \cdot \varepsilon_0 \cdot \sigma_0 T \geq 1 \quad (1)$$

- As limiting case in single-event analysis we assume that the probabilities of the event to be true or accidental should be equal. The single event registered should be accidental with the probability less than 50%. This is the second condition.

$$n_{\text{true}} \geq 0.5 \geq n_b \quad (2)$$

As long as all background is produced by the beam, the number of events  $n$  registered by the detector and the corresponding rates  $R$  in the detector are proportional to each other.

$$n_i = T \cdot N_d \cdot R_i \quad (3)$$

with  $T$  the measuring time and  $N_d$  the number of subdivisions (pixels) of the total detector area. We divide (2) by  $N_d T$ , and obtain an equation between rates.

$$R_{\text{true}} \geq (2TN_d)^{-1} \geq R_b \quad (4)$$

- The rate of random events  $R_b$  of a sequence of  $K$  subsequent signals in fixed order simulating a decay chain of  $(K - 1)$  generations is given by the product of the rates in the  $K$  classes of signals and the  $(K - 1)$  correlation times ( $t$  between the decay events [20]). This rate equation is the third condition.

$$R_{bi} = \prod_{i=1}^K R_i \cdot \prod_{i=1}^{K-1} \Delta t_{i,i+1} \quad (5a)$$

Equation (5a) holds for events starting with an implanted nucleus of the 1st generation, followed by a fixed order sequence of  $(K - 1)$  generations of subsequent signals. As random sequences are reversible in time, in case of chains ending with a rare and unambiguous spontaneous fission signal, also counting in reversed order of time is possible and equivalent.

Replacing the fixed order of time by a free order of the signals following the leading sf-event, we obtain:

$$R_{bK} = \prod_{i=1}^K R_i \cdot \prod_{K-1}^1 \Delta t_{K,i} \quad (5b)$$

The  $(K - 1)$  correlation times of the sequence define a mean correlation time.

$$\overline{\Delta t} = \left( \prod_{i=2}^K \Delta t_{i,j} \right)^{(K-1)^{-1}} \quad (6)$$

The mean correlation times for a fixed (5a) and partially free order (5b) are different.

Equations (5) are rate equations, which do not depend on the measuring time  $T$ . Only smaller rates and smaller correlation times in the  $(K-1)$  generations reduce the random rate. Underlying  $R_b$  are the cross sections  $\tau_i$  and decay times  $\tau_i$  of the beam-induced processes making up the rates  $R_i$  together with the efficiencies  $\tau_i$  of the experimental facility to suppress the different species indexed  $i$ .

#### 4.1 The maximum possible correlation times

Besides the number of random events the above equations determine also the maximum possible correlation times of an experiment given. Combining (4) and (5) gives,  $R_b = (\overline{\Delta t})^{K-1} \prod_{i=1}^K R_i \leq (2TN_d)^{-1}$  and it follows:

$$2(\overline{\Delta t})^{K-1} n_j \prod_{\substack{i=1 \\ i \neq j}}^K R_i \leq 1 \quad (7)$$

Equation (7) defines a maximum value of  $t_{\max}$  which fulfills the limiting case of (4).

$$t_{\max} = \left( \frac{R_b^{\max}}{\prod_{i=1}^K R_i} \right)^{(K-1)^{-1}} = \left( 2n_j \prod_{\substack{i=1 \\ i \neq j}}^K R_i \right)^{-(K-1)^{-1}} \quad (7a)$$

This largest possible correlation time to find the event to be true with a 50% probability is given by the rates  $R_i$  and the corresponding rate of random events  $R_b^{\max} = (2N_d T)^{-1}$ . Or, in other words, the number of starters of sequences  $n_j$  and the rates in the  $(K-1)$  generations  $R_i$  fix  $t_{\max}$ . For  $n_j$  the class of signals with the smallest number of events should be chosen, that is spontaneous fission, if observed. Further, we assume that for each class of signals  $i$  the rates  $R_i$  are mean values averaged over the total measuring time  $T$  for a pixel given. For a homogeneous distribution of particles across the detector area the rates  $R_i$  of a class of signals  $i$  for all pixels should be about the same and  $R_i$  is the average over all of them.

The rates can be related to cross sections if, as e.g. in the reactions  $^{48}\text{Ca}$  on  $^{248}\text{Cm}$ , all the cross sections were measured [15].

$$R_i = \frac{n_i}{N_d \cdot T} = \frac{L}{N_d} \cdot \varepsilon_i d\Omega \cdot \frac{d\sigma_i}{d\Omega} \quad (8)$$

with  $n_i = L\varepsilon_i d\Omega T \frac{d\sigma_i}{d\Omega}$  and  $\varepsilon_i = S_i^{-1}$

$n_i$  is the total number of signals in the class  $i$  registered in the detector during the measuring time  $T$ ,  $L$  the luminosity,  $d\Omega$  the angular acceptance of the spectrometer, and  $\varepsilon_i$  is the efficiency to transmit the particle  $i$  through the separator and to find it ready to enter the detector system. The inverse of  $\varepsilon_i$  equals the suppression  $S_i$  of particles of class  $i$  by the spectrometer. The luminosity per pixel  $L/N_d$  scales all classes of signals induced

by reactions in the target. The largest possible correlation time to find a true event  $t_{\max}$ , is expressed by the cross sections  $\sigma_i$ ,  $L/N_d$ ,  $d\Omega$ , and the efficiencies  $\varepsilon_i$ .

$$t_{\max} = \frac{N_d}{Ld\Omega} \left( 2n_j \prod_{\substack{i=1 \\ i \neq j}}^K \frac{d\sigma_i}{d\Omega} \varepsilon_i \right)^{-(K-1)^{-1}} \quad (7b)$$

A high luminosity  $L$  and a large opening angle of the spectrometer  $d\Omega$  reduce the maximal possible correlation time, a fact not to be forgotten in the run for higher beam currents and opening angles in order to reach ever lower cross sections. The acceptance angle should be chosen not larger than the angular width of the distribution of fusion evaporation residues  $d\Omega_0$ . Segmenting the detector into a high number of pixels  $N_d$  and suppressing the unwanted species by the spectrometer are tools helping to reach larger correlation times.

Target recoils and transfer products having passed the spectrometer at the ion optical field settings for the expected fusion evaporation residues are assumed to be suppressed by the same factor. Moreover, transfer products are a source of spontaneous fission events and of  $\alpha$ -activity in the energy window defined in the search. If  $\varepsilon_i$  is replaced by one suppression factor in the spectrometer common to all classes of signals  $i$ , (7b) transforms to:

$$t_{\max} \leq \frac{N_d}{L\varepsilon d\Omega} \left( 2n_j \prod_{\substack{i=1 \\ i \neq j}}^K \frac{d\sigma_i}{d\Omega} \right)^{-(K-1)^{-1}} \quad \text{with } \varepsilon = S^{-1} \quad (7c)$$

Reactions with small cross sections  $\sigma_i$  for spontaneous fission and  $\alpha$ -particles in the window produce less accidentals. Using Pb and Bi targets and avoiding actinide targets, if possible, is of advantage. Accidental correlations in “cold fusion”-reactions with  $d\Omega_0$  smaller, no fission and less  $\alpha$ -particles from transfer products are easier to be handled than in “hot fusion” and  $^{48}\text{Ca}$ -induced reactions. The target recoils are inevitable. They occur in the beam pulses and start random sequences. Besides suppression by the spectrometer the different kinematics of binary reactions allow their further suppression. The best method is energy-discrimination in the implantation detector. Time-of-flight discrimination is less effective as most of the particles passing the spectrometers have either equal velocities as in SHIP, or a wide velocity distribution covering all masses as in gas-filled separators.

To calculate the minimum possible correlation time, (7a) should be used after having been modified in the following. The condition of (1,2), that one chain is detected and the decision on this chain, whether true or accidental, can be taken on the basis of a 50% probability, is an unrealistic assumption [21]. The times  $t_{\max}$  calculated from (7a) derived with this assumption are too large. The time constants  $\lambda_0$  of the exponential decay rate for the true events and the time constant  $\lambda_b$  of the Poisson-distribution characterizing the correlation times of the background events are equal for the assumed case of a 50% probability to find a true event. To discriminate the

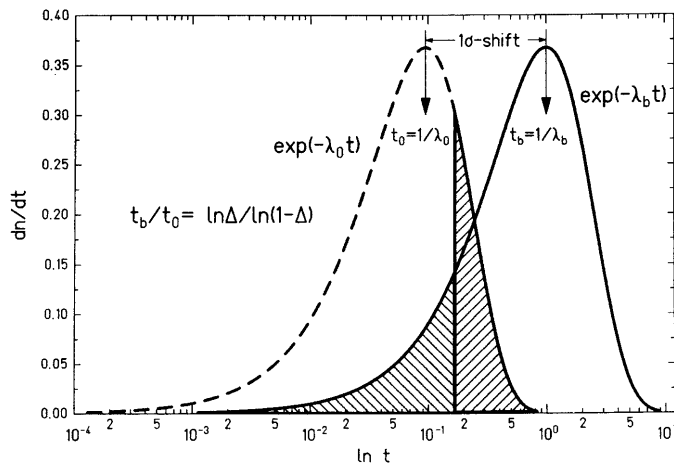


**Fig. 1.** Distribution of time differences in a Poisson-distributed background or in an exponential radioactive decay. For single-event analysis in the limiting case that the event is random or true with a 50% probability, a distance of a factor 10.5 corresponding to the  $1\sigma$ -width of the distribution should be kept between the investigated radioactive decay constant  $\lambda_0$  and the Poisson-distributed correlation times of the background characterized by  $\lambda_b$ . The maximum possible correlation times for an experiment should be kept smaller by at least this factor for all applications

true events the maximum possible correlation time should guarantee, that the event is true within a  $1\sigma$ -probability. The shortest correlation times of the random distribution occurring in the exponential decay ( $\lambda_b$ ) up to a probability of 16% the largest correlation times of the distribution of true events ( $\lambda_0$ ) occurring up to a probability of 84% define the distance for a  $1\sigma$ -interval (68%) between the two distributions, Fig. 1. The distributions are separated in their time constants by a factor of 10.5. This follows for exponential decays from  $\lambda_b/\lambda_0 = \ln \Delta / \ln(1 - \Delta)$  with  $\Delta = 0.16$ , the 16%-probability of the interval borders. At least a  $1\sigma$ -margin of safety of a factor 10.5 should be taken. The  $2\sigma$ -margin would be a factor of 30.2. We reduce  $t_{\max}$  calculated from (7a) by the factor of 10.5.

$$t_{\max}^{1\sigma} = \frac{1}{10.5} \cdot \frac{1}{\left(2n_K \prod_{i=1}^{K-1} R_i\right)^{(K-1)^{-1}}} \quad (7d)$$

## 4.2 The “figure-of-merit” to suppress accidentals

Replacing in (7c)  $n_j$  by  $(L \cdot \varepsilon d\Omega \cdot T) \left(\frac{d\sigma_j}{d\Omega}\right)$  an expression for  $t_{\max}$  is obtained separating the nuclear input of background reactions, as the cross sections  $\left(\frac{d\sigma_j}{d\Omega}\right)$ , from the parameters characterizing the separation facility, as the luminosity  $L$ , the suppression of binary reaction products  $\varepsilon^{-1}$ , the acceptance  $d\Omega$ , the number of pixels  $N_d$  in the detector, and the measuring time  $T$ .

$$t_{\max} = \frac{N_d}{L\varepsilon d\Omega} (L\varepsilon d\Omega T)^{-(K-1)^{-1}} \left(2 \prod_{i=1}^K \frac{d\sigma_i}{d\Omega}\right)^{-(K-1)^{-1}}$$

Searching with different facilities for a single event from the same reaction characterized by the values of  $\sigma_0$  and  $\sigma_i$ , we find that the maximum correlation time  $t_{\max}$  defines for a given facility a “figure of merit”  $Q$ , which classifies their correlation abilities.

$$Q \equiv \frac{N_d}{L\varepsilon d\Omega} (L\varepsilon d\Omega T)^{-(K-1)^{-1}} \quad (9a)$$

For large values of  $K$  the “figure of merit” reduces to:

$$Q = \frac{N_d}{L \cdot \varepsilon \cdot d\Omega} = \frac{S/d\Omega}{L/N_d} \quad (9b)$$

$Q$  is the ratio of the suppression of target-like recoils and transfer products emitted into a unit of solid angle over the luminosity per pixel-detector. It is valid for the best case, that is counting  $\alpha$ -particles in the pauses of a discontinuous cycle. For measuring in the continuous mode, the  $Q$ -values must be reduced by factors of (10–30). The  $Q$ -values cannot be improved by longer measuring times.

## 4.3 The error probability of single correlated events

For single decay chain analysis  $n_b$  degenerates to the probability  $P_{\text{err}}$  of the true event not to be true.  $n_b = 1$  means the event is accidental. For  $n_b = n_{\text{true}}$  the probabilities the event to be true or random are equal and both are 50%. Down at  $n_b \leq 0.1$  one can seriously start to speculate on an eventual new non-random phenomenon indicated by the correlation with a probability to be true of larger than 90%.

The number of random events follow from  $n_b = R_b \cdot N_d \cdot T$  applied to the two cases for the random rates, (5a,b). We obtain the number of random events.

$$n_{bi} = n_K \prod_{i=1}^{K-1} R_i \cdot \prod_{i=1}^{K-1} \Delta t_{i,i+1} \quad \text{for fixed order} \quad (10a)$$

Equation (10a) does not depend on the time direction chosen for the analysis. Seen from the recoil- or from the sf-signal  $n_{bi}$  is the same.

$$n_{bk} = n_K \prod_{i=1}^{K-1} R_i \cdot \prod_{i=1}^{K-1} \Delta_{K,i} \quad (10b)$$

for partially free order, sf-decays leading

The time differences  $\Delta t_{K,i}$  are different, whether the event is analyzed starting with the recoil- or the sf-signal.

## 5 Applications to the discussed experiments

Table 1 compares SHIP83 (II), the FLNR gas-filled separator [7], and the FLNR separator VASSILISSA [8, 9]. The quantities in brackets refer to the ratios compared to experiment (II). The minimum accessible cross section  $\sigma_{\min}$ , and the “figure-of-merit”  $Q$  to suppress accidentals are the decisive quantities to be compared for the different separating facilities and experiments.

**Table 1.** Specifications for different separation facilities used for  $^{48}\text{Ca}$  beams on heavy actinide targets. The minimum cross section  $\sigma_{\min}$  and the maximum correlation time  $t_{\max} = \text{const.} \cdot Q$  are the most important quantities characterizing a facility and an experiment.  $Q$ -values given hold for large values of  $K$ , that is for long chains

	GSI SHIP83 [6]	FLNR gas-filled sep. [7]	FLNR Vassilissa [8, 9]
Target/mg $\text{cm}^{-2}$	0.4 ( $^{248}\text{Cm}$ )	0.37 ( $^{244}\text{Pu}$ )	0.2 ( $^{242}\text{Pu}$ ); 0.3 ( $^{238}\text{U}$ ) [8]
$L/\text{b}^{-1} \text{h}^{-1}$	$1.6 \cdot 10^9$	$5.9 \cdot 10^9$ (3.7)	$4.2 \cdot 10^9$ (2.6)
$\varepsilon_0$	0.25	0.40 (1.6)	0.30 (1.2)
T/h	250, pause/pulse=2	816 (3.3)	768 (3.1)
$\sigma_{\min}/\text{pb}$	10	0.5 (0.05)	0.9 (0.09)
$\sigma_{\text{recoil}}^{\text{enter}}/\text{mb}$	1.1	4.1 (3.7)	4.8 (4.4)
$\varepsilon$	$2 \cdot 10^4$	$2 \cdot 10^{-5}$ (0.1)	$5 \cdot 10^{-5}$ (0.25)
$d\Omega/\text{msr}$	2.2	8.6 (3.9)	10 (4.5)
$N_d$	120	240 (2)	600 (5)
$Q_{K \gg 1}$	1	1.4	1.7
$Q_{K \gg 1}^{\text{pause}}$	1	0.14	0.17

**Table 2.** Data used from [7–9] to calculate the maximum possible correlation times and error probabilities for the sequences found.  $\Delta t_{i,i+1}$ -intervals larger than the maximum possible correlation times are given as bold numbers

Ref.	GSI SHIP83 [6]	FLNR gas-filled sep. [7]	FLNR Vassilissa [9]	[8]
K	5 (hypoth.)	5	3	2
$n_{\text{sf}}$	1	2	2	2
$n_{\text{recoil}}$	$5.6 \cdot 10^4$	$2.5 \cdot 10^5$	$1.7 \cdot 10^6$	$2.5 \cdot 10^6$
$R_{\text{recoil}}/h^{-1}$	2.8	1.3	4	5.4
$R_{\alpha}/h^{-1}$	0.03 (pause)	1	1; (3 for escape)	–
$R_{\text{sf}}/h^{-1}$	$3 \cdot 10^{-5}$	$1 \cdot 10^{-5}$	$4 \cdot 10^{-6}$	$4 \cdot 10^{-6}$
$\Delta t$ -intervals/min, start sf-signal	–	16.5–1.6–15.4–0.5	9.4–1.3 s	3
$t_{\max}^{1\sigma}/\text{min}$	13.9 (pause)	3.7	4.1–14 s	0.9
$\Delta t_{\text{sf}/i}/t_{\max}^{1\sigma}$	–	4.5	0.8	0.17
$n_{b_i}^{\text{up } 1\sigma}$	–	4.5	7.9	9.7
$n_{b_i}^{\text{up } 1\sigma}$	–	$< 5 \cdot 10^{-4}$	$< 9 \cdot 10^{-3}$	$< 1.1$
$n_{b, \text{sf}}^{\text{up } 1\sigma}$	–	$< 0.72$	$< 0.77$	$< 1.1$

## 5.1 The minimum accessible cross section

The larger luminosities of a factor of 3–4 and the longer measuring times of factors 3 explain the lower cross section limits obtained today at FLNR compared to GSI in 1983. The same cross section limits as at FLNR are obtained now at SHIP94 [3] and at LBL Berkeley [4]. 1 pb as a limit has become state of the art.

As the efficiencies  $\varepsilon_0$  for all instruments are approaching one and the target thickness is restricted by the technique of separating the recoils in-flight, the only possibility to increase the sensitivity of the separating facilities is, besides the triviality of longer measuring times, an increase of the beam intensity. Most solid targets are now at the limit given by the energy deposited in the target, and the targets start to melt down. Improvement of cooling or the use of continuously renewed targets, as gaseous or vapour targets, have been envisaged, in order to reach cross sections in the sub-pb regime.

## 5.2 The “figure-of-merit” to suppress accidentals

The “figure-of-merit” is calculated for large  $K$ -values. Table 1 gives the relative values of  $Q$  normalized to experiment (II) for the two modes of irradiation, continuous or discontinuous. The improvement for the FLNR instruments is marginal for the continuous beam mode. The higher suppression factors of background reactions achieved are nearly cancelled by the larger acceptances of the spectrometers. Certainly, the suppression of background events in the detector system by making use of the different kinematics of fusion and binary reactions can still be improved in the future. Over the years, the luminosity per pixel  $L/N_d$  could be kept nearly constant by increasing the segmentation of the detectors, thus compensating the decrease in  $Q$  by the higher luminosity. The most efficient way to boost  $Q$  is to stay with timely separated irradiation and counting cycles. The experiment (II) run in the discontinuous mode [6], had a (6–7) times larger  $Q$ -value than the more recent experiments (I) run in

the continuous mode. The discontinuous mode compared to the continuous mode loses luminosity, but this loss gains an increased capacity of suppression of accidentals. It depends on the lifetimes of the isotopes investigated, whether the increase of the luminosity can be exploited and the experiment can be run in the continuous mode, or it is a better choice to decrease the random rate by lowering the luminosity per pixel and introducing a discontinuous irradiation cycle in order to assure a detection of true events at all.

### 5.3 The rates for the different classes of signals

The number of sf-events and the rates  $R_i$  are given in Table 2, as presented in [6–9]. These rates are needed to calculate the maximum correlation times  $t_{\text{max}}$  and the number of random events. The production cross section known for a class of signals, the rate can also be calculated using (8) with the values  $L$ ,  $N_d$ ,  $\varepsilon$ , and  $d\Omega$  given in Table 1 for the different instruments. Using actinide targets in  $^{48}\text{Ca}$ -reactions we have to live with the cross sections producing fission isomers ( $\sim 200$  nb) and transfer products with  $\alpha$ -energies larger than 8 MeV in the energy window of superheavy nuclei ( $\sim 0.6$  mb). The cross section for target recoils produced by Rutherford back scattering of the projectile is  $d\sigma/d\Omega = b^4/4$  with  $b/fm = 0.144Z_1Z_2/E_{\text{c.m.}}$ . At the Coulomb barrier in  $^{48}\text{Ca}/^{248}\text{Cm}$ -collisions  $d\sigma/d\Omega = 0.48b$  is obtained.

The expected number of elastic recoils dominates the recoil rate. Only 3% are contributed by transfer products. The rates for the elastic recoils reproduce within a factor of 2 measured recoil rates. This is within the error applied to measured rates and cross sections using the recoil-separator technique. As the measured rates are reproduced for the three instruments, the suppression factors  $\varepsilon^{-1}$  for the different instruments given in Table 1, seem to be realistic.

The cross section of fission isomer production allows another test of consistency. Multi-nucleon transfer products are emitted anisotropically in forward direction. In the measurement, [15], all transfers were captured in a cone of  $\pm 60^\circ$  opening angle. With an isomer ratio of  $10^{-4}$ , a number of two sf-decays observed in experiment [7], and a total cross section for  $^{244}\text{Am}$ -production of 2 mb, we find a cross section of 0.4 pb to register spontaneous fission in the detector. Moreover, we confirm the strong forward directed flow into a cone of restricted angles ( $\pm 30^\circ$ ), as seen in [15].

Assuming that all transfer products, like the fission isomers, are emitted anisotropically in forward direction into this cone, and that the  $\alpha$ -emitters producing  $\alpha$ -energies in the selected energy window of (8.1–11) MeV for superheavy elements have a total cross section of 0.6 mb, [15], we estimate a rate of  $\alpha$ -particles in the window of  $3.1 \cdot 10^{-2} \cdot h^{-1}$ . This rate is smaller by a factor of 32 compared to the rate of  $1 \cdot h^{-1}$  measured in the experiment [7]. The large rate of  $1 \cdot h^{-1}$  in the continuous beam mode points to the presence of another mechanism producing

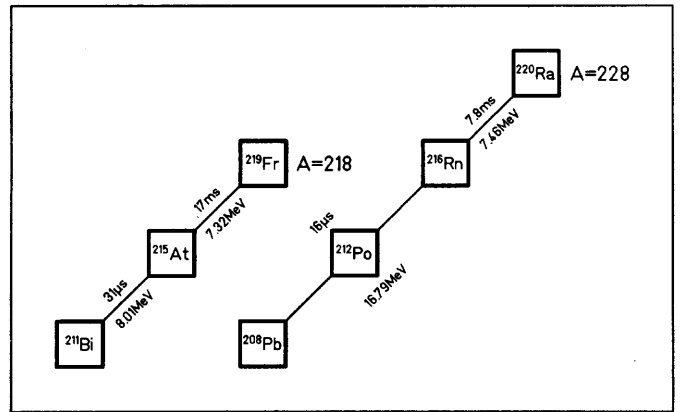


**Fig. 2.** Correlation chains found in the 1983 SHIP-experiment (II) for the transfer products  $^{219}\text{Fr}$  and  $^{220}\text{Ra}$  [16]

signals besides the  $\alpha$ -decays of transfer products. The  $\alpha$ -decays from transfer products can be measured well in the pause. In experiment (II) a pulse/pause ratio of  $\alpha$ -rates was measured equal to the ratio of the above measured and calculated rates. We conclude that the beam produces a background of fake  $\alpha$ -particles, the energies of which are in the window. No TOF-signal was registered, nor did they penetrate into a veto-detector behind the implantation detector. The high rate of such particles during the pulse neither in the experiments (I) nor in experiment (II) is well investigated. Fast protons or  $\alpha$ -particles produced in the reaction or by elastic recoil in the gas volume of the gas-filled separators, are a working hypothesis. They are transmitted through the separators, but their energy-loss signals in the time-of-flight detector are too small to induce a signal there. In the main implantation detector their energy-loss signals are larger and fall in the window preset for  $\alpha$ -particles from superheavy elements. The fast light particles can be partly eliminated by a veto-detector behind the implantation detector. Recoils correlated to the fake  $\alpha$ -particles are no correlations to  $\alpha$ -particles with well defined energies emitted by transfer products.

Elastic target recoils and transfer products having entered into the separator and being transferred to the detector give TOF-signals and signals in the implantation detector. They produce random correlations. For short correlation times also true correlations between transfers and their  $\alpha$ -decays can be observed. This was shown in experiment (II). Figure 2 shows complete  $\alpha$ -decay chains of transmitted transfer products found in the  $^{48}\text{Ca}/^{248}\text{Cm}$ -irradiation for  $^{219}\text{Fr}$  and  $^{220}\text{Ra}$ , respectively [16]. Figure 3 shows the scatter-plot of  $\alpha$ -decays correlated to implanted ions in the time ranges of  $13 \mu\text{s}$  to 40 ms for  $\alpha$ -particles emitted during the accelerator pulse (8 ms) and to 312 s for  $\alpha$ 's during the pauses between accelerator pulses (12 ms), [22]. In the energy range of (7–15) MeV and a mass range of  $A = (100 - 400)$  the different groups are separated. At  $A = 220$  true correlations of transfer products with their  $\alpha$ -particles are obtained in the energy range (7–12) MeV, e.g. the isotope  $^{214}\text{Po}$  (164  $\mu\text{s}$ ) produces the events at 7.69 MeV. Abundantly we find ran-

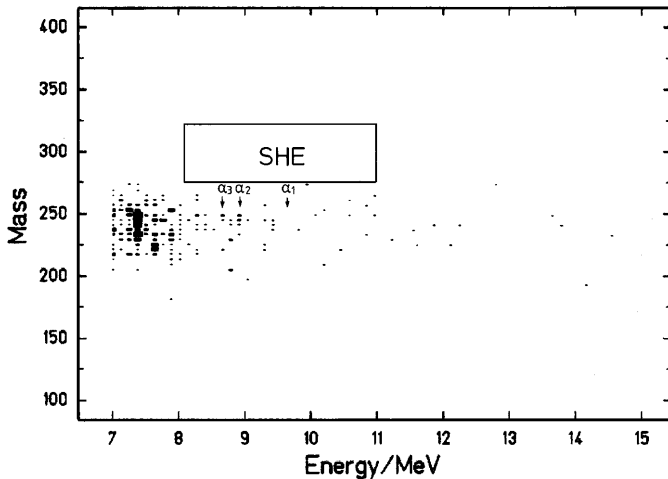


**Fig. 3.** Correlation plot for time and position correlated implanted ions and  $\alpha$ -decays. Position window  $\pm 0.8$  mm, time windows: from  $13 \mu\text{s}$  to  $40$  ms for decays during UNILAC-beam-bursts, to  $312$  s for decays in the beam pause [22]. The 3  $\alpha$ -energies observed in experiment [7] and the region where superheavies are expected, are indicated. Most of the  $\alpha$ -correlations observed in experiment (II) are randomly correlated to elastic  $^{248}\text{Cm}$  recoils or  $\alpha$ -emitting transfer products in the mass range  $A = 211$ – $220$ . True correlations were established for times smaller than  $7$  ms

dom correlations between target-recoils ( $A = 248$ ) and  $\alpha$ -particles from transfer products all over the whole energy range. The signals at  $7.31$  MeV mostly from  $^{219}\text{Fr}$  ( $21$  ms) and its predecessors, and from  $^{223}\text{Th}$  and  $^{225}\text{Pa}$  are the most abundant group. A mass discrimination towards the high masses of eventual superheavy elements in the detector system by their kinematics is possible. In the  $2\sigma$ -window around the superheavy fusion evaporation residues ( $A = 293$ ), no event was found at a mass resolution of about  $10\%$  FWHM. The dose collected for Fig. 3 in experiment (II) was about  $8\%$  of the dose accumulated in experiment [7]. In the energy window of  $(8.1$ – $11)$  MeV chosen for experiment [7],  $42$  correlations between target recoils and  $\alpha$ -particles from transfers were observed. The emitters  $^{213}\text{Rn}$  ( $8.09$  MeV),  $^{213}\text{Po}$  ( $8.38$  MeV),  $^{214}\text{Fr}$  ( $8.45$  MeV),  $^{215}\text{Rn}$  ( $8.67$  MeV),  $^{212}\text{Po}$  ( $8.78$  MeV), and  $^{211}\text{Po}$  ( $8.88$  MeV) can be identified. As emitters with halfives shorter than  $2 \mu\text{s}$  were not resolved,  $\alpha$ -energies in the range of  $(16$ – $17)$  MeV were observed resulting from summing of two consecutive  $\alpha$ -decays. If one of these  $\alpha$ -particles escapes and is not registered with its full energy, all energies between  $(9$ – $11)$  MeV can be observed due to a summing of a full energy pulse with an escape peak,  $(0.5$ – $2)$  MeV. Random correlations of recoils to  $\alpha$ -particles from transfer products were registered in experiment (II) and reveal the  $\alpha$ -spectrum of transfer products. Assuming the “ $\alpha$ -rate” in the continuous mode is mainly carried by fast light particles, the spectrum observed is continuous and lines from transfer products are suppressed. A diagram corresponding to Fig. 3 showing recoil- $\alpha$ -correlated spectra for  $K = 2$ -,  $K = 3$ -, and  $K = 4$ -sequences would certainly help to better understand the continuous beam

experiments, the so-called “ $\alpha$ -rates” of which are particles without TOF-signal, but only in their minority  $\alpha$ -particles from radioactive decays.

#### 5.4 The maximum correlation times

With the measured rates and the numbers of spontaneous fission decays in Table 2, maximum possible correlation times  $t_{\text{max}}$  are calculated for the three separating facilities. For experiment (II) a hypothetical  $K = 5$ -sequence in a discontinuous irradiation mode is assumed. For the experiments (I) a  $K = 5$ -sequence and a  $K = 3$ -sequence are chosen, corresponding to the published sequences in [7] and [9], respectively.

The uncertainties in the measured quantities entering the calculation of  $t_{\text{max}}^{1\sigma}$  using (7d) additionally have to be taken into account. The small numbers of 1 or 2 correlated events based on the observation of spontaneous fission in the FLNR-experiments (I) introduce large errors [20]. Moreover, all rates entering (7d) have absolute uncertainties of a factor of 2. The mean standard-errors are calculated. The values of  $t_{\text{max}}^{1\sigma}$  at the lower standard-error limit are considered as a safe value of the maximum possible correlation time.

The values of  $t_{\text{max}}^{1\sigma}$  at its lower standard-error limit are given in Table 2. For a continuous beam mode all the instruments considered for the reactions investigated are restricted to correlation times smaller than  $4$  min. This value is far from the reported value of  $1$  h [9]. For  $K = 5$ -sequences the FLNR gas-filled separator performs best with  $t_{\text{max}}^{1\sigma} = 3.7$  min. However, the experiment (II) run in the discontinuous mode would have reached  $t_{\text{max}}^{1\sigma} = 14$  min for a hypothetical  $K = 5$ -sequence.

The observed times between a fission event and a first preceding signal are related to the maximum possible correlation time by the ratio  $\Delta t_{\text{sf},i}/t_{\text{max}}^{1\sigma}$ , which is given in Table 2. On the average, the three experiments have seven times longer observed correlation times than the maximum possible correlation times, which allow to select a true event within a  $1\sigma$ -margin. The time criterion  $\Delta t_{\text{sf},i} \leq t_{\text{max}}^{1\sigma}$  is not fulfilled by any of the recent FLNR experiments (I) claiming discovery of superheavy elements. For comparison the experiment [10], which we used to establish the “One Atom / One New Element”-method, was reevaluated under the same conditions as described. The value of  $\Delta t_{\text{sf},\alpha} \leq t_{\text{max}}^{1\sigma}$  is  $2.2 \cdot 10^{-3}$  with  $t_{\text{max}}^{1\sigma} = 1.6$  h. This event was a  $K = 4$  sequence with  $2$   $\alpha$ -decays and a sf-decay, all of them in irradiation pauses.

## 6 The error probabilities

In order to evaluate the error probabilities of the five sequences presented in experiments (I), the rates of the different classes of signals, as presented in [7–9], are given in Table 2. Moreover, the uncertainties of the numbers of leading signals, rates, and correlation times determine



the standard-error of these probabilities. The probability  $n_b^{\text{up}1\sigma}$  at the upper standard-error limit, is considered as a safe limit for  $n_b$ . A corresponding lower value for the probability that the single event observed is true,  $p_{\text{true}} = (1 - n_b^{\text{up}1\sigma})$ , follows. The error of  $n_b$  is very large, as the numbers of leading signals in the case of spontaneous fission are only 1 or 2. The distribution of the correlation times for a single event observed is given in Fig. 1. The width of this distribution determines the fluctuations of the correlation times. In the case of single events the upper standard-error of each of the correlation times is a factor of 5.79. Finally, all the rates are only known within a factor of 2. For the  $K = 5$ -sequence observed in the  $^{244}\text{Pu}$  irradiation [7] the range of  $n_b$  from the lower to the upper value of its standard-errors has a width of a factor of 64.  $n_b$  and the upper value  $n_b^{\text{up}1\sigma}$  differ by the large factor of 11. For each of the five sequences the mean standard errors are calculated using the errors for small numbers given in [20].

Analyzing the sequences ending with a spontaneous fission signal, we learn from (5), that the rate of random events, which is proportional to the product of the rates for the  $K$ -classes of signals, become small in case the spontaneous fission rate enters the product. This rate compared to all other rates is smaller by a factor of  $10^5$ . It is the occurrence of fission in the experiments (I) which pulls the number of random events below  $n_b = 0.5$ .

In the following, the sequences presented in [7–9] are disentangled. The number of random events  $n_{bk}^{jn} = n_j \prod_{i=j+1}^n R_{j+1} \cdot \Delta t_{j,j+1} \dots R_n \cdot \Delta t_{j,n}$  is presented with  $K = |j+1-n|$  the number of signals in the sub-sequences,  $j$  the leading class of signals, and  $n$  the class of signals terminating the sequence. The correlated sequences for the  $K = 5$  event observed in the  $^{244}\text{Pu}$  irradiation [7] and the two  $K = 3$  events observed in the  $^{242}\text{Pu}$  irradiation [9] are presented in Table 3. The values of  $n_{bk}^{jn}$  are presented in squares with  $(K-1)^2$  boxes. Sequences in fixed order of correlation times, (10a), are presented in the upper right boxes of the square and sequences in partially free order and backward direction in time, (10b), in the lower left boxes. The  $K = 2$ -sequences which are independent of the time-flow are in between in the diagonal of the square. There are two numbers given for each sequence. The first number  $n_{bk}^{jn}$  is calculated using (10a,b). The second number is the corresponding value  $n_b^{\text{up}1\sigma}$  at the upper standard-error limit. We find large numbers of random events in all sequences started by recoils and terminated by “ $\alpha$ -particles”. Unless there is an sf-event in the sequence, the sequence is random. Sequences built on an sf-signal running backward in time are found in the last row, (10b). They are the choice giving spontaneous fission the importance, it has for the finding of non-random events. All values of  $n_{b, sf}^{\text{up}1\sigma}$  are larger than 0.5. The  $K = 5$ -sequence gives the minor probability of 28% that the sequence might be true. Correspondingly, the mean value of the probabilities for the two events in the  $^{242}\text{Pu}$ -experiment is 23% [9]. For the  $^{238}\text{U}$  experiment the proba-

**Table 3.** The random event numbers  $n_{jn}^{bk}$  of sequences of  $K = (j+1-n)$ -signals starting with class  $j$  and ending with class  $n$  signals calculated for the parameters given for the  $K = 5$ -sequence observed in the  $^{48}\text{Ca}/^{244}\text{Pu}$  irradiation [7], upper square, and the two  $K = 3$ -sequences observed in the  $^{48}\text{Ca}/^{242}\text{Pu}$ -irradiation [9], lower two squares. The first number is  $n_b$ , the second number is  $n_b^{\text{up}1\sigma}$ , that is  $n_b$  at its upper standard-error limit.  $r = \text{recoil}$ ;  $\alpha_1, \alpha_2, \alpha_3 = \alpha$ -particles;  $\text{sf} = \text{spontaneous fission}$ . The modes of analysis in the upper right part of the squares follows a fixed order in time, whereas in the lower left part of the squares a partially free order in time with the  $\text{sf}$ -event leading is presented

$K = 5$ sequence ( $^{244}\text{Pu}$ , [7])			
r- $\alpha_1$ -2	r- $\alpha_2$ -3	r- $\alpha_3$ -4	r-sf-5
$2.1 \cdot 10^3$	540	14	$4 \cdot 10^{-5}$
$1.4 \cdot 10^4$	$4.8 \cdot 10^3$	150	$5 \cdot 10^{-4}$
$\alpha_2$ -r-3	$\alpha_1$ - $\alpha_2$ -2	$\alpha_1$ - $\alpha_3$ -3	$\alpha_1$ -sf-4
$1.8 \cdot 10^4$	$5.1 \cdot 10^4$	$1.3 \cdot 10^3$	$3.8 \cdot 10^{-3}$
$1.5 \cdot 10^5$	$3.3 \cdot 10^5$	$1.2 \cdot 10^4$	$4.1 \cdot 10^{-1}$
$\alpha_3$ -r-4	$\alpha_3$ - $\alpha_1$ -3	$\alpha_2$ - $\alpha_3$ -2	$\alpha_2$ -sf-3
570	$1.5 \cdot 10^3$	$5.3 \cdot 10^3$	$1.5 \cdot 10^{-2}$
$5.8 \cdot 10^3$	$1.3 \cdot 10^4$	$3.4 \cdot 10^4$	0.13
sf-r-5	sf- $\alpha_1$ -4	sf- $\alpha_2$ -3	sf- $\alpha_3$ -2
$6.8 \cdot 10^{-2}$	$9.1 \cdot 10^{-2}$	0.16	0.55
0.72	0.90	1.4	3.6
Two $K = 3$ sequences ( $^{242}\text{Pu}$ , [9])			
r- $\alpha_1$ -2	r-sf-3	r- $\alpha_1$ -2	r-sf-3
623	$4.6 \cdot 10^{-4}$	$2 \cdot 10^4$	$6.1 \cdot 10^{-3}$
$2.5 \cdot 10^3$	$2.6 \cdot 10^{-3}$	$8.2 \cdot 10^4$	$3.4 \cdot 10^{-2}$
sf-r-3	$\alpha_1$ -sf-2	sf-r-3	$\alpha_1$ -sf-2
0.19	0.31	0.10	0.38
0.99	1.3	0.55	1.6

bilities are negligibly small. Following (10b) all sequences are random.

The number of random events for the  $K = 2$ -sequences between the recoil and the following “ $\alpha$ -particle” are of the order of  $10^4$  for all the three reported events, as is seen from the upper left boxes of the squares. For the five fission events the direct correlations between the fission signal and the preceding recoil signal are given in each of the lower right boxes. The probabilities  $n_b^{\text{up}1\sigma}$  are by far larger than 0.5. An average of  $n_b^{\text{up}1\sigma} = 1.7$  together with a mean ratio  $\Delta t_{sf,i}/t_{\text{max}}^{1\sigma} = 7$  (see Sect. 3.4) show that the spontaneous fission signals for all five events are randomly correlated to their recoil signals. Recoil- $\alpha$  correlations as well as sf-recoil correlations for  $K = 2$ -sequences are all random.

In the upper right corner of the squares of Table 3 the time order is fixed and we notice the  $n_b$ -values become smaller. The upper right box shows the  $K = 5$ -sequence starting with an implanted recoil and ending in spontaneous fission. This is the analysis chosen in [7, 9] for the three  $\alpha$ -correlated events. It gives for the three sequences at the upper standard-error limit probabilities that the

**Table 4.** The random event numbers  $n_b$  for the sequences observed in experiments [7–9] for the 2 cases, (10a,b), and the case of decoupled sf-events. The first number gives the random event number, the second number the random event number at the upper standard-error limit

Ref.	[7]	[9]	[8]	Comment
$K$	5	3	2	
$n_{sf}$	2	2	2	
$n_{bi}$	$4 \cdot 10^{-5}$	$1.7 \cdot 10^{-3}$		fixed order
$n_{bi}^{up1\sigma}$	$5 \cdot 10^{-4}$	$9.4 \cdot 10^{-3}$	–	
$n_{b,sf}$	$6.8 \cdot 10^{-2}$	0.14		Partially free order, backward in time, sf-leading
$n_{b,sf}^{up1\sigma}$	0.72	0.77		
$n_b$	0.55	0.34	0.28	$K = 2$
$n_b^{up1\sigma}$	3.6	1.4	1.15	sf-events decoupled from sequence

event is true larger than 99.95% [7], 99.7%, and 96.6% [9]. The small values of  $n_b$  can be traced back to the short correlation times between the recoil and the first following “ $\alpha$ -particles” of 30 s [7], 1.32 s, and 14.4 s [9]. The decisive point for the randomness of the correlations is the question whether these small time differences between recoils and a following “ $\alpha$ -particle” found at times of 34 min, 9.4 min, and 4.1 min before the sf-event, are still of relevance. The large numbers of accidentals between recoils and “ $\alpha$ -particles” even for large values of  $K$  never approach the value of  $n_b = 0.5$ . Their correlations alone are far from being true. The small probabilities obtained for the full sequences between the starting recoil signal and the terminating sf-signal alone do not prove a true event chain. If, as discussed before, for the long correlation times to the sf-event decoupling had occurred, the link between the sf-event and the sequence is broken. Building on recoil-correlated sequences in spite of decoupling is not allowed, and discovery of a new isotope or a new element cannot be concluded.

In Table 4 the probabilities for the sequences reported in experiments (I) to be random, are given. The values following an analysis using (10a,b), presented in the upper right and lower left corner in the squares of Table 3, respectively, are given. Together with the values for the decoupled sf-events presented in the lower right corner of the squares. In case of the  $K = 2$  sequences of experiment [8] all three evaluations converge to a same number. For experiments [8, 9] a mean value for each of the two sequences observed is given.

We summarize the findings on error probabilities.

- The fixed order in time analysis gives  $n_b$ -values which are small and indicate large probabilities, that the sequences might be true.
- The partially free order in time analysis with the sequence looked at in backward direction of time, starting with the sf-events shows  $n_b$ -values, which still could indicate that the sequence might be true. However, at the upper standard-error limit the probabilities are

larger than 0.5. On the average, the sequences at this safe limit have a probability to be true of only 25%.

- The correlation times between the sf-event and its preceding signal are larger by a factor of 7, compared to the maximum possible correlation times for the experiments. The sequences of signals are decoupled from the sf-events. The  $n_b$ -values between 0.28 and 0.55 giving a mean value of 0.4 are very close to the limit of 0.5. All values at the upper standard-error limit indicate that the sequences are random.
- The correlation analysis gives no support to the conclusion of experiments (I) to have discovered superheavy elements.

## 7 Conclusions

The recent FLNR-experiments bombarding the targets  $^{238}\text{U}$  [8],  $^{242}\text{Pu}$  [9], and  $^{244}\text{Pu}$  [7] by  $^{48}\text{Ca}$ -projectiles do not prove the formation of the superheavy isotopes  $^{289,287}\text{114}$ ,  $^{285,283}\text{112}$ ,  $^{281}\text{110}$  and  $^{277}\text{Hs}$ , as claimed in the recent publication in Nature [9]. The arguments against the claim are summarized in the following.

Two assumptions, which could have been checked experimentally before any experiment started, lack any proof. One of them concerns the necessary performance of the equipment for decay-chain analysis. The other one concerns the question, whether the reaction cross-sections would be large enough in order to detect the envisaged superheavy elements by the available facility.

- The statement in [9] that the FLNR-facilities measure true time correlations between signals from particles registered in their detector system up to 1 hour lacks any experimental verification. It is an ad-hoc assumption. The power of experimental facilities to suppress accidentals can be compared by a “figure-of-merit”, which is proportional to the segmentation of the detector and the suppression of reaction products others than the wanted fusion evaporation residues, and inversely proportional to the luminosity of the experiment and the opening angle of the spectrometer. The performance to avoid random sequences in the experimental facilities used at FLNR-Dubna with their higher luminosities and opening angles, and the continuous irradiation mode introduced into the field for the first time, is inferior to the facilities used by the GSI group before [6]. The method to detect one single decay sequence and to prove the existence of a new isotope [10] is restricted in the continuous irradiation mode to correlation times of a few minutes. The capability to correlate 1 hour-decay chains could have been demonstrated by the detection of chains of four generations from 31-min  $^{226}\text{Th}$  to  $^{214}\text{Po}$  transmitted to the detector with an effective cross section of about  $1 n_b$ .
- The trend towards experimentally smaller cross sections was established. In many fusion reactions [3, 11, 12] The ratio of Coulomb to surface energy disrupting the combined system increases steadily with

the atomic number, and decreases the fusion probability in the entrance channel. Until now, no experiment was presented that isotopes of any actinide fuse with projectiles beyond  $^{34}\text{S}$ . Neither Ar- nor Ca-isotopes have been successfully used in fusion reactions with actinides before. Why should the cross section between  $^{34}\text{S}/^{238}\text{U} \rightarrow ^{272}\text{Hs}$  and  $^{48}\text{Ca}/^{244}\text{Pu} \rightarrow ^{292}114$  over a range of six elements stay constant? The small shell-correction energy of a few MeV for  $^{48}\text{Ca}$  is said to change the survival probability in the evaporation cascade. The experiments [7–9] were done with the assumption that  $^{48}\text{Ca}$ -projectiles in 3-n reactions break the trend to smaller cross-sections. This assumption lacks support by any independent experiment performed inside or outside FLNR. In the reaction  $^{232}\text{Th}(^{36}\text{Ar},4n)^{264}\text{Hs}$  an isotope is produced, the decay-chain of which is known. Its cross-section could have been measured, and it would have given a starting point for further explorations towards higher atomic numbers.

The analysis of the FLNR-experiments showed [7–9]:

- All rates measured for incoming recoils classified by their signals in a TOF-detector, and of “ $\alpha$ -particles” classified not having produced a signal in this detector are larger by a factor of at least 105 compared to the rare fission events, of which one signal was registered every 15 days. Five observed fission events are the essence of the three experiments performed.
- The total kinetic energies of these fission events were measured. The energy ( $190 \pm 10$ ) MeV is consistent with fissioning elements between Cm and Fm, but too small for the proposed spontaneous fission of  $Z = 112$  and Hs.
- The sequence of signals correlated to the five fission events should be analyzed in time backwardly, as the fission signals are the only solid base in the flood of registered signals. The times to the next preceding signal for the five events are in the range of (0.9–16.5) min. An experiment performed at a given facility is restricted by a longest possible correlation time, for which non-random correlations are possibly to be found. For all three experiments discussed these times are shorter than the corresponding above correlation times. The correlations between the fission events and their preceding signals, recoil or “ $\alpha$ -particle”, are random.
- The conclusion in papers [7–9] to have observed non-random sequences is based on an analysis of the sequences starting with a recoil signal and terminating with a fission signal. For the sequence of 5 signals the first “ $\alpha$ -particle” is registered 0.5 min after the registration of the recoil signal [7]. For the two sequences of 3 signals the first “ $\alpha$ -particles” are found 1.3 s and 14 s after the registration of the recoil signal [9]. These times are short compared to the correlation times seen from the sf-signals (34 min for the sequence of five signals, and 9.4 min and 4.1 min for the two sequences of three signals). It is this ratio of the two correlation times of nearly two orders of magnitude which

makes the random probabilities strongly dependent of the mode of analysis. The authors of experiment (I) have chosen the mode giving the smallest possible values of the random probabilities. The justification of a linkage over the long total times of the sequences depends on the hypothesis of the 1 hour-correlation time.

- As we demonstrated, the short time correlations between recoils and “ $\alpha$ -particles” are decoupled from the much longer correlation times of the spontaneous fission events, and an analysis of the sequence starting with the recoil signal carries no information on the fission events. The correlation analysis assigning the 5 fission events and their preceding signals to superheavy elements, as proposed in [7–9], cannot be maintained. The 5 fission events are uncorrelated. Moreover, their measured total kinetic energies are too low for the superheavy elements discussed. No supporting argument for a possible production of superheavy elements in the  $^{48}\text{Ca}$ -induced reactions investigated survives. The evidence that any superheavy isotope or element has been discovered in the FLNR experiments must be classified as “very weak”, and the claim of discovery of new isotopes and a new element must be rejected.

I acknowledge fruitful discussions with M. Bernas, W. Bröchle, F.P. Hessberger, M. Leino, M. Schädel, K.H. Schmidt, and H.-J. Specht. My special thanks go to S. Lüttges for her help in shaping the manuscript.

## References

1. P. Armbruster *Ann. Rev. Nucl. Part. Sci.* **35** (1985) 135
2. G. Münzenberg *Rep. Progr. Phys.* **51** (1988) 57
3. S. Hofmann *Rep. Progr. Phys.* **61** (1998) 639
4. V. Ninov *PRL* **83** (1999) 1104
5. Yu.A. Lazarev et al. *PRL* **73** (1994) 624 and Yu.A. Lazarev et al. *PRL* **75** (1995) 1903
6. P. Armbruster et al. *PRL* **54** (1985) 406
7. Yu. Oganessian et al. *PRL* **83** (1999) 3154
8. Yu. Oganessian et al. *EPJ* **A5** (1999) 63
9. Yu. Oganessian et al. *Nature* **400** (1999) 242
10. G. Münzenberg et al. *Z. Phys.* **A315** (1984) 145
11. K.-H. Schmidt and Morawek W. *Rep. Progr. Phys.* **54** (1991) 949
12. P. Armbruster *Ann. Rep. GSI 1998, GSI-1999-1* p.8 and *Rep. Progr. Phys.* **62** (1999) 465
13. Yu.A. Lazarev *Ann. Rep. FLNR 1991/92, Dubna 1992* p. 203
14. M. Schädel et al. *PR* **C33** (1986) 1547
15. H. Gäggeler et al. *PR* **C33** (1986) 1983
16. P. Armbruster et al. *Ann. Rep. GSI 1983, GSI-1984-1* p. 81
17. J. Tke et al. *Nucl. Phys.* **A440** (1985) 327
18. W.Q. Shen et al. *Phys. Rev.* **C36** (1987) 115
19. A. Türler *Phys. Rev.* **C46** 1364 (1992)
20. K.-H. Schmidt et al. *Z. Phys.* **A316** (1984) 19
21. K.-H. Schmidt et al. *Nucl. Phys.* **A318** (1979) 253
22. Y.K. Agarwal et al. *Ann. Rep. GSI 1983, GSI-1984-1* p. 79